

Graph percolation as an analog to granular force networks

John F. Wambaugh

*Departments of Physics and Computer Science and Center for
Nonlinear and Complex Systems Duke University, Durham, NC 27708**

(Received April 20 2006)

A remarkable feature of granular materials is the distribution of force along intricate networks. Even regular inter-particle contact networks produce wildly inhomogeneous force networks where certain “chains” of particles carry forces far larger than the mean. We examine experimentally obtained granular force networks using an algorithm to obtain a force network graph that we can analyze to gain insight into its structure. We then compare our observations with the results for different models, including random bond percolation in which the structure of the graph is captured by a single parameter p — the chance of the presence of a bond. Our findings suggest that the mean behavior of geometry-intrinsic force network quantities may be captured by graph descriptions.

PACS numbers: 81.05.Rm,05.10.-a,89.75.Hc,89.75.Da

I. INTRODUCTION

Granular materials are composed of many particles interacting by contact. In a dry granular material only contact forces are present — there are no long-range and no cohesive forces. Without knowing the assembly history of a granular material, the mobilization of the friction of each contact is indeterminate. Thus, even materials composed of macroscopically uniform particles, such as spheres, display a highly non-uniform contact network. Even when neglecting friction, any differences in the size of particles, including microscopic aberrations on the surface of “smooth” spheres, is sufficient to create a complicated network of contacts [1].

A. The Contact Network

For any configuration of grains (for example, Fig. 1.1) if the position and shape of each grain is known then a contact network can be generated describing the contact between grains.

The equations describing a granular material can be grouped into the known equations describing the behavior of the individual grains and the unknown equations describing the contacts between the grains as a function of material assembly and history. These unknown equations can be cast as undetermined relationship between inter-grain forces and the geometry of the contact network [2].

Attempts to resolve the indeterminacy of the constitutive relations have focused upon statistical approaches similar to thermodynamics. Ideally, it might be possible to determine aggregate properties of granular materials that do not depend upon knowing the specifics of the grains to arbitrary precision. Unfortunately there are two problems that have made such an approach non-trivial. First, a granular material at rest is only in a quasi-equilibrium. An arbitrarily small addition of energy can cause irreversible (plastic) rearrangement of the material. This is in part due to the second problem, the lack of an analog to temperature to “thermalize” the system. The actual energy due to temperature is far too small to move grains, and there is no other quantity allowing the material to explore phase-space for lower energy states.

Despite, or perhaps because of, these problems statistical approaches to granular materials continue to be developed. One such approach is that of Edwards and Oakeshott (1989), who determine the “Edwards Entropy” from considering the number of possible quasi-static configurations of a granular material within a fixed volume. In this formulation, volume takes the place of energy for statistical considerations and a replacement for temperature, the *compactness*, is introduced as a measure of the “fluffiness” of the material [3, 4].

Satake (1985) explored representing the contact network as a graph embedded in real space with a vertex at the center of each grain and an edge for each contact. Satake was able to define such mean quantities as the fabric, stress and strain tensors for a granular material using the contact network graph and an auxiliary graph. The auxiliary graph contains a set of edges representing potential contacts. In two dimensions the auxiliary graph is constructed by

*Electronic address: wambaugh@phy.duke.edu

adding to each polygon of edges additional edges of smallest possible length to create triangles of edges. The fabric, stress and strain tensors represent the average number of contacts in a particular direction, the average force the average displacement in response to those forces respectively.

The contact network is not static. In response to an anisotropic applied stress the number of contacts increases in the direction of the stress. Satake was able to include this effect in the mean behavior but not get the actual distribution of forces upon the graph [5].

B. Force Networks

Other approaches to granular materials focus on force propagation. The fluctuations in the magnitude of the force carried by a single particle within a granular material have been observed to extremely large in both experiments and simulations. This is the result of long-range force correlations brought about by the presence of a *force network* in which some bonds of the contact network carry forces much larger than the mean force on all the contacts. As in Fig. 1.2, forces are seen to propagate along roughly linear “chains” of contacts. Because the force network depends upon the contact network, the propagation direction and distribution of the chains depends strongly upon the history of the granular material [6, 7].

Contact and force networks are considered *fragile*. Though they can be very rigid in response to stress in the direction of the bonds, bond friction will only support small tangential forces before the force chains break and the contact network possibly rearranges [8]. Whereas the forces within a cohesive material usually cluster about some mean, the distribution of forces in a force network is roughly exponential indicating the possibility for extremely large forces. Since tangential forces are not supported, their distribution falls monotonically, while forces along the chains are peaked at a mean value before falling exponentially [9].

If the force network cannot support the granular material, the material will rearrange until the instant the new contact and force network supports the granular material. Granular materials may perhaps be thought of as existing in a *critical state*, in which the force network behaves as an order parameter in response to displacements of the material [1]. Usually the force network is determined using a threshold — only bonds carrying forces larger than some value, often the mean force, are considered to be part of the force network. In such a case, the force network may not be rigid itself because it will not contain some bonds that, while carrying only small amounts of force, provide rigidity to the network. Simulations have observed a critical-like transition from sparsely distributed network of force chains to a percolating network as a function of of a intergrain mobilization of friction threshold [10].

II. MICROSCOPIC MODELS OF GRANULAR MATERIALS

There have been many attempts to model the behavior of force networks, most famously the “ q -Model” of Copper-smith (1996). In the two-dimensional q -Model, depicted in Fig. 2, granular materials are represented as a lattice of sites with two upward neighbors and two downward neighbors. Each site has an intrinsic weight that is added to any weight it receives from the neighbors above it. The total weight on a site is distributed between the two downward neighbors with one receiving a fraction q of the total weight and the other receiving $1 - q$. The q -Model allows the determination of the distribution of weight by working downwards from the top of the lattice. This process can be shown to be diffusive-like in the continuum limit [11].

Diffusive systems, however, do not allow for long-range propagating forces like those seen in force networks. Experiments have shown that even averaging over multiple force chain networks does not support a diffusive description of granular materials [12].

In the case where q is allowed to only take the values of 1 or 0, the q -Model does show chain-like clusters of bonds. In the infinite lattice limit the distribution of weights on the sites becomes a power-law. This case will be referred to as the “critical q -Model” [11].

In all cases the q -model is a “scalar” model in that the distribution of weight, not force is being described. The forces exerted upon a particular lattice site do not need to balance, and this in part explains the lack of chain-like structures in all but the critical case. “Vector” models that attempt to include force balance also exist. The simplest lattice model with force balance is the “tripod” model that, in two-dimensions, assigns each site three downward neighbors, one directly below and two offset to either side by a fixed angle. In the continuum limit this model can give wave-like equations for propagating stress [13]. Additionally, other models have included torque-balance on each site, giving meaning to the finite extent of the grains [14]. Including both force and torque balance allows derivation in simple cases for equations describing force equilibrium as functions of the contact distribution [15].

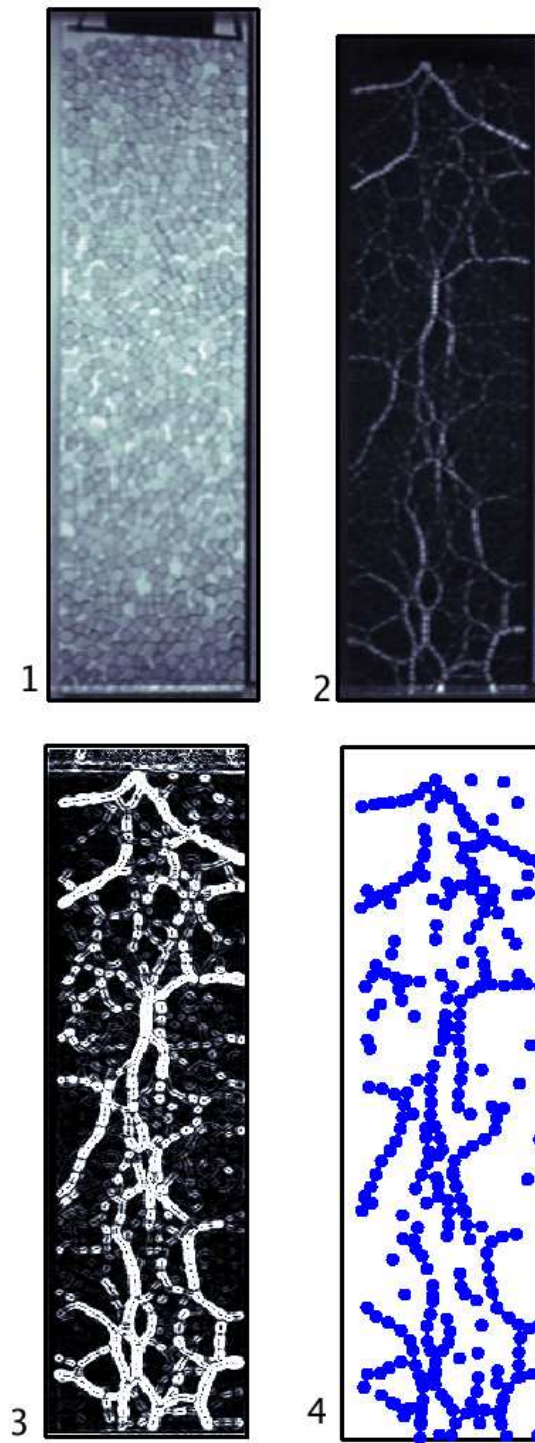


FIG. 1: Analysis of the two-dimensional granular assembly of bi-disperse polymer disks depicted in **1**. The contact network for the disks can be thought as a series of vertices centered at each disk connected by edges wherever two disks are in contact. **2** Because the disks are photoelastic, when they are illuminated between crossed polarizers bright fringes appear in disks under stress allowing force chains to be clearly seen. A load has been applied to the top of the pile causing the creation of additional contacts and force chains supporting the load. **3** We examine the gradient of the photostress image as a rough measure of the number of fringes in each disk, which is proportional to the applied force. **4** Finally, we apply an algorithm to the gradient image to find a graph describing the force network.

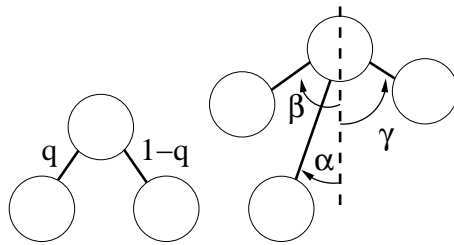


FIG. 2: **Left** In the two-dimensional q -Model, a fraction q of the total weight on a particle on a regular lattice is transferred to one lower neighbor, and the remaining $1 - q$ is transferred to the other. As originally formulated by Coppersmith, et al., the values of q can be drawn randomly from different distributions. In the “critical” case, the value of q is limited to either 0 or 1. **Right** To make rough analogy to the q -Model for more complicated geometries, we use a geometry-based q -Model in which the fraction of a vertex’s weight that is distributed along a downward pointing edge is proportional to the sine of the angle that edge forms with the vertex.

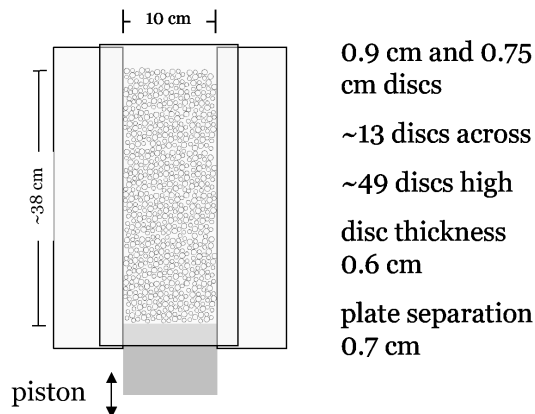


FIG. 3: Experimental setup for observing granular force networks. Bi-disperse disks made of a photoelastic polymer are confined vertically to two-dimensions between clear plastic sheets and illuminated between crossed polarizers. The fringes induced by applied stress on each grain are imaged with a CCD camera.

III. RANDOM BOND PERCOLATION ON A GRAPH

Research into the general behavior of force networks in granular material has shown that certain properties, including the exponential distribution of large forces, should be expected to arise regardless of the grain-scale model. In other words, it may be that the properties of granular materials are phenomena of the statistics of force networks, and not the micromechanics of the grains [16, 17].

This insight has led to approaches to granular materials from the mesoscopic level. By assuming the presence of force chains and describing their behavior, it may be possible to avoid some of the complexity of granular materials and still achieve meaningful results [18, 19]. In particular, network approaches to granular materials may bear fruit because the statistical mechanics of networks are beginning to be understood [20].

The critical q -model is similar to random bond percolation on a lattice. Percolation theory provides a framework for understanding how small clusters of connected sites aggregate into larger clusters as a function of the probability that a bond is selected. There are well known values, depending upon the geometry of the lattice, for transitions from loose aggregates of clusters to system-spanning, “infinite” clusters [21]. In the case of the critical q -model, bonds are selected at random from a set of edges representing the connections between the lattice sites with the restriction that each lattice site has only one load-bearing downward bond. The set of load-bearing bonds can be thought of as a subset of edges that, with the vertices as the lattice sites, forms a sub-graph of the contact network. In this way, cluster size corresponds to weight and thus the distribution of cluster sizes gives bounds on the distribution of weights in an analytic manner since weight at a given vertex is equal to one plus the size of the tree rooted at that vertex.

Though no fixed lattice of contacts exists in disordered granular materials, the contact network may instead be thought of as a random graph. In general, random graphs are composed of a set of vertices connected by a random subset of all possible edges selected by a probabilistic rule. Random graphs are very attractive from a statistical

point of view because their mathematics is well known. Probability generating functions can be determined for the formation of clusters of edges and the bounds can be set for the distribution of cluster sizes [22, 23].

Random graph approaches predict exponential, Poisson-like distributions for the number of contacts at each vertex. Attempts to use random graphs to understand other physical networks have been rejected in the past because of the tendency of other networks to display the “small world” phenomena — a power-law distribution of contacts [24, 25]. Since the distribution of contacts in granular materials are constrained between the minimum necessary to support the particle and the maximum allowed by particle geometry, it is therefore reasonable to examine whether random graph approaches might still be suitable. Very recently, the fractal Apollonian Network of edges has been suggested as a graph description of the contact network since it meets the requirements, of Euclidean geometry, exhibits power-law behavior and is still be subject to graph-theoretic analysis [26]. Other work has suggested that granular force networks belong to a specific universality class, and that distributions of forces in a wide range of isotropic granular systems can all be scaled onto a single distribution [27, 28]. It is worthwhile to evaluate whether experimentally-obtained granular force networks may be thought of as random graphs constructed from edges in the contact network. Characterization of the graph-intrinsic properties of these networks may allow for the construction of analytic graph theoretic descriptions of mean force network behavior.

IV. OBTAINING FORCE NETWORKS

We use the experimental setup depicted in Fig. 3 to observe force networks within actual granular matter. We confine 650 bi-disperse photoelastic polymer disks within a vertical, two-dimensional silo. Photoelastic materials show bright fringes of light in proportion to the stress applied to the material. By taking the gradient of an image of a photoelastic disk along multiple directions we effectively “count” the number of fringes and, using a linear calibration from data, can obtain the force distribution throughout the granular material (see Fig. 1.3).

Using the gradient image of a particle force network we convolve with the image of one stressed grain to locate the positions of all stressed grains in the image. These positions are treated as a two-dimensional embedding of vertices.

We then assign an edge between all vertices separated by a distance in the range of $l/4$ to l where l is a tunable parameter that has been chosen so that the graphs correspond to the force network. The lower range is necessary because some fringe patterns within a single disk produce multiple points when convolved. This has the effect of artificially increases clustering of the graph.

The specific values of the network-finding parameters used depends upon many properties of the images of force networks, including the image resolution and dispersion of the disks. These parameters, in addition to the correlation threshold for locating vertices, must be tuned to produce force network graphs that accurately describe force networks. The distributions reported here do not change unexpectedly with variation of parameter values, and in particular, the distribution of cluster sizes does not vary significantly.

Adding an edge to any grain that already has the threshold value k_{max} edges causes the longest edge to that vertex to be removed. We use the smallest k_{max} that does not significantly alter $P(k)$. The set of vertices and edges found this way are the experimentally obtained force network (see Fig. 1.4).

Using ensembles of force networks under various loads, we can determine the probability distribution function for the average number of contacts per vertex and number distribution of cluster sizes. We can also record the observed force at each vertex and create an ensemble probability distribution for force.

As shown in Fig. 4, there are several quantities that can be measured for any given graph. In addition to cluster size and vertex degree, one can measure the size of the upward tree rooted at each vertex. The upward tree is a graph made by treating each edge as a directed edge oriented against gravity. The size of the upward tree corresponds to the number of vertices who are at least partially supported by a given vertex. As illustrated in Fig. 2, weights can be assigned to each vertex and propagated along each downward pointing edge in proportion to the cosine of the angle each edge makes with the vertex. This allows for a q -Model-like weight distribution to be generated for non-lattice geometries. For all of these quantities an aggregate probability density function is calculated.

We analyzed one hundred force networks obtained from experimental images of our grains under a 56 g overload. Fig. 5 shows the distribution of vertex degrees and, as expected for chain-like structures, most vertices have two edges. From geometric considerations, the maximum number of contacts for a single disk in a bi-disperse mixture of disks with radii r_{small} and r_{large} is $k_{max} = \pi/2 / \arcsin[r_{small}/2 / (r_{small} + r_{large})]$. In this case $k_{max} = 6.85$ and there is no probability of seeing a vertex with degree higher than six. Thus, as Fig. 5 shows, the imposed cutoff of $k_{max} = 5$ used in the edge finding routine does not significantly affect the distribution of $P(k)$ since fewer than a tenth of all vertices have degree larger than 4.

The critical nature of granular force networks is apparent in Fig. 6. The distribution of number of observed clusters of size s (as a fraction of the total number of clusters) appears to follow a power law, although the distribution is very

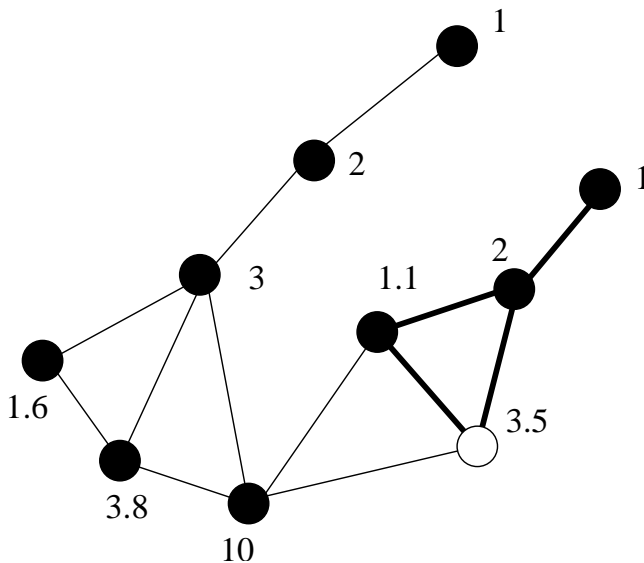


FIG. 4: Illustration of the graph quantities measured. The cluster size $s = 10$ includes all the vertices. The size of the upward tree rooted at the white circle (indicated by thicker edges), $t = 4$ includes all vertices connected by upward edges only. The degree of the white node is $k = 3$. The numbers indicate approximate geometric q -Model weights w , determined for each vertex by assigning each an inherent unit weight and distributing the weight among all downward edges in proportion to the sine of the angle each edge makes with the vertex.

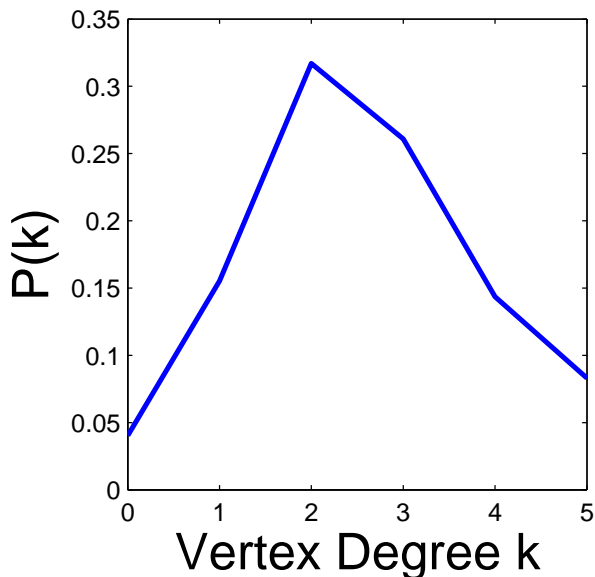


FIG. 5: In the distribution of vertex degree there is a peak at $k = 2$ corresponding to the majority of vertices participating in chains. The lack of a sharp uptick at $k = 5$ indicates that truncating at 5 has not significantly affected the distribution. These results are from analyzing one hundred experimentally-obtained force networks under 56g load.

noisy at cluster sizes approaching the size of the system. This behavior lends support to the suggestion of Roux, et al. that the force network may be an example of a self-organized critical phenomena.

Figure 7 shows the probability distribution of intensity of the gradient squared image at the pixel location of each vertex. The intensity corresponds with the force on the disk at that vertex and thus Fig. 7 is the force probability distribution. The probability is found to fall faster than a power law. Also, there is a clear mean value larger than the value for a single disk.

Distributing forces along the force network as if using the q -Model gives the distribution seen in Fig. 8. The q -Model weights are sub-power law, but show a monotonic decrease unlike that of the actual force data. The distribution of

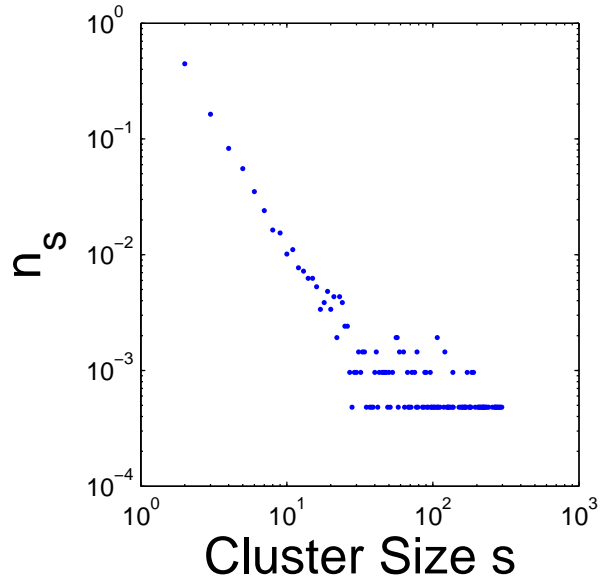


FIG. 6: The distribution of n_s , the number of clusters of size s divided by the total number of clusters, appears to be roughly linear over many decades of probability and one decade of cluster-size (corresponding to the system size). A power-law distribution would support the idea of Roux et al. that the force network may perhaps be considered a critical phenomenon. These results are from analyzing one hundred experimentally-obtained force networks under 56g load.

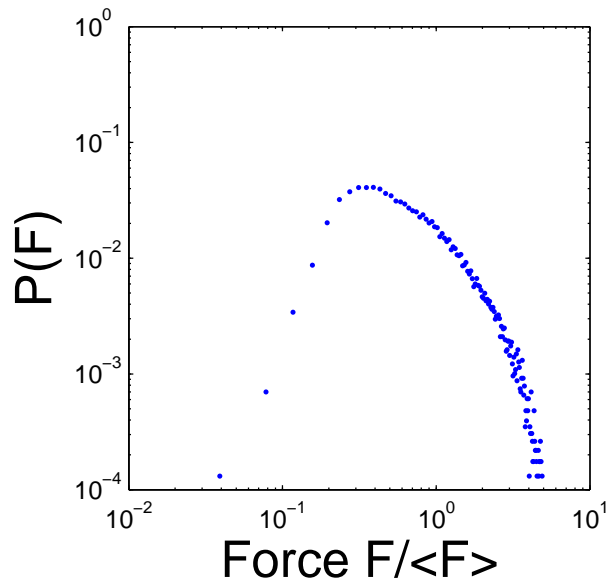


FIG. 7: The force observed at each vertex computed from the gradient is non-monotonic — the least-stressed particles are below the mean force for particles in the network. These results are from analyzing one hundred experimentally-obtained force networks under 56g load.

upward tree sizes for the experimentally-obtained networks was found to be too noisy to draw meaningful conclusions. The distribution was very roughly linear however, with a shallower slope than that of overall cluster sizes. The relative shallowness of the slope was at least consistent since since one large cluster may contain many large trees.

The geometric limit of 6 possible contacts per disk corresponds to 6 potential edges per vertex, however the average number of contacts (coordination number) for a disordered granular material is 4 [1]. Assuming that there are four contacts per vertex, we can calculate a chance p that a bond carrying a large force is present. For a particular vertex i , $p_i = k_i/4$ and the average value $p \equiv \sum_{i=1}^N p_i/650 = \sum_{i=1}^N k_i/4/650$, where N is the total number of vertices in

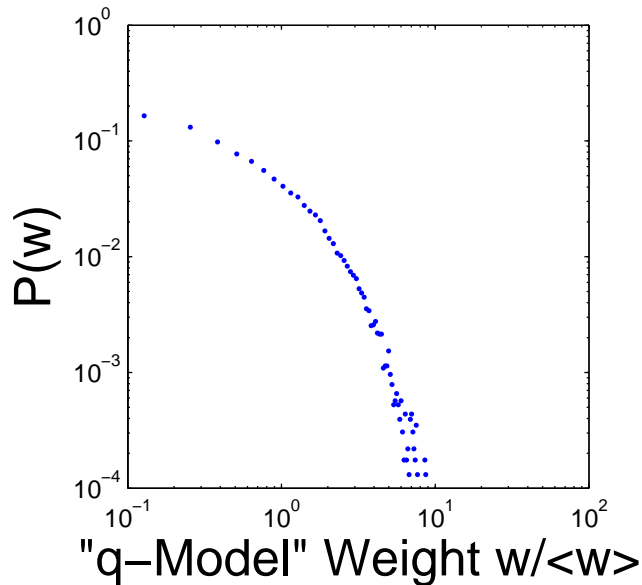


FIG. 8: The probability density function of weight assigned to vertices in the experimentally-obtained force networks by a method similar to the q -Model. Unlike the actual force data, the curve is monotonic. These results are from analyzing one hundred experimentally-obtained force networks under 56g load.

the force network graph, and 650 is the total number of particles. For the observed networks, $p = 0.2214$. This is below the critical percolation probability $p_c \approx 0.3473$ necessary for a system-spanning, infinite cluster on an infinite triangular lattice [21]. Thus we see many non-percolating force networks.

For each vertex we can also compute the cluster coefficient — how many edges are shared by the neighboring vertices $\binom{4}{2}$ possible edges. We calculate $c = 0.1219$ for the observed force network. This amount of clustering is similar to that seen in small-world networks that exhibit power law behavior, such as the WWW and power grids [25]. However, because of the finite extent of the particles our calculation assumes a restricted number of contacts per particle. This is different from a true random network where any vertex may be contact with an unlimited number of other vertices at any position. Thus it is clear that this is not a perfect analogy.

Finally, since we expect 4 contacts on average, Fig. 5 indicates that grains in the force network are typically in contact with one or two grains not in the force network. This indicates interplay between the force network and the contact network at every particle.

V. COMPARISON WITH MODELS

Having characterized the behavior of actual force networks, it is possible to make comparisons to simple models. Using 500 realizations of the critical q -Model on a 10×40 vertex hexagonal grid (chosen to reflect the aspect ratio and roughly the number of vertices in our experiments) as in Fig. 9.1, it was possible to determine distribution functions for vertex degree, cluster size, upward tree size and weights assigned by the q -Model.

In addition to the q -Model results, random graphs were also constructed from a set of edges arranged in one of two hexagonal configurations — one where in addition to downward-angled edges there were horizontal edges (see Fig. 9.2), and one where there were vertical edges (Fig. 9.3). For each random graph a subset of these edges were chosen with a probability p . With six possible edges per vertex, the triangular lattice is similar to the bi-disperse system though angular distributions are severely restricted.

A range of different p values were examined for both triangular orientations. In addition to the $p = 0.2214$ that was determined experimentally, we examined values of $p = 0.15$ and $p = 0.3$ above and below the measured p . Finally, we examined $p = 0.5$, a value greater than the percolation threshold, $p_c = 0.3473$, for a system-spanning cluster in an infinite triangular lattice and equal to the value of frictional mobilizations at which Matsuoka observed a transition to infinite clusters.

The distributions of vertex degree for 500 realizations of the critical q -Model and triangular lattices with different bond probabilities are shown in Fig. 10. Since the q -Model has to give chain like structures, it is not surprising to

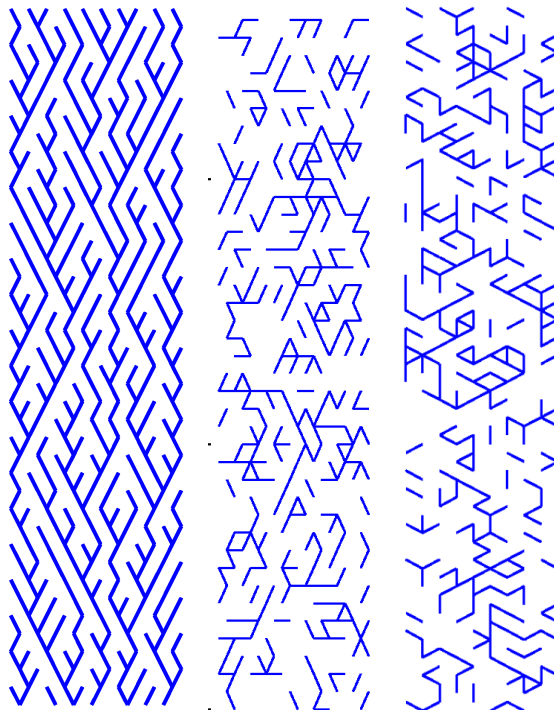


FIG. 9: From left to right: **1** An instance of the q -Model in the critical case. **2** A random graph ($p = 0.25$) composed of edges from a hexagonal lattice oriented horizontally. **3** A random graph ($p = 0.25$) composed of edges from a hexagonal lattice oriented vertically.

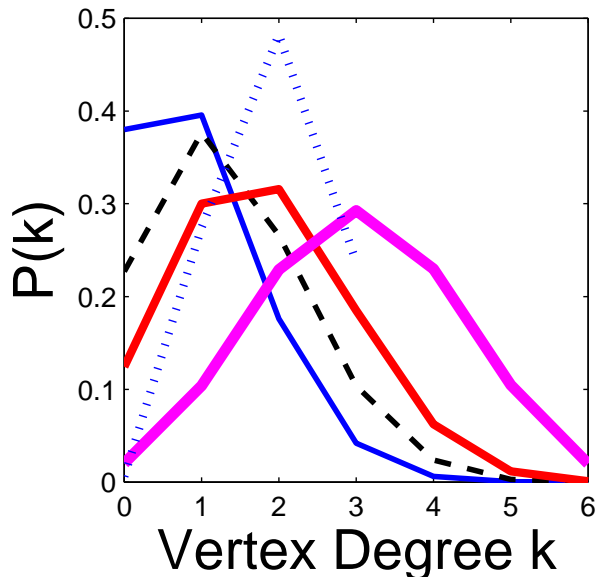


FIG. 10: The probability density function for degree vertex from analyzing 500 realizations of critical q -Model and random triangular graphs. The critical q -Model is indicated by a dotted line. Dashed lines indicate random graph results for the experimentally obtained $p = 0.2214$. Solid lines of increasing weight indicate $p = 0.15, 0.3$ and 0.5 respectively. While the q -Model by design gives the expected peak at $k = 2$ — indicating chain-like structures, the best match to Fig. 5 by a random graph is for the slightly larger than observed $p = 3$. All the random graphs give a better distribution of higher vertex degree values since in the critical case of the q -Model $k \leq 3$. For random graphs vertex degree is independent of whether the basis is oriented horizontally or vertically.

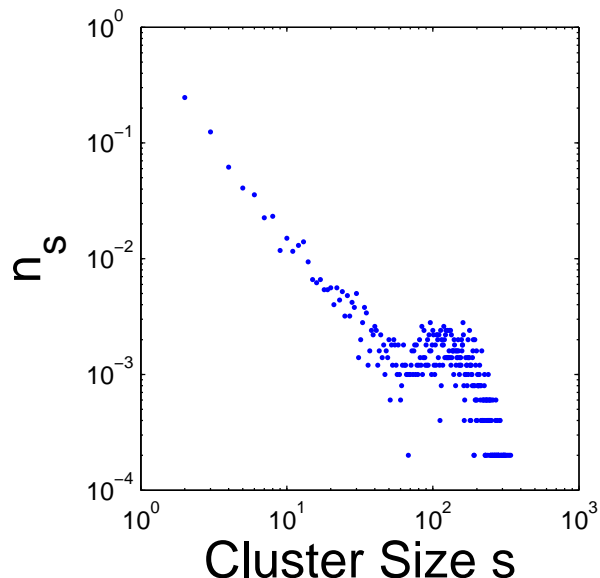


FIG. 11: The distribution of number of clusters of size s from analyzing 500 realizations of the critical q -Model. On a log-log plot the distribution of smaller clusters is linear, but there is a peak at large cluster sizes. This peak differs from the behavior of random bond models and is due to the requirement in the critical q -Model that each site have only one downward neighbor by having tuned the model to create long chains of contacts we have increased the number of large clusters.

see that $P(k)$ peaks at $k = 2$, indicating that most elements are members of a single chain. For a random graph constructed with the bond probability $p = 0.2214$ calculated from our experimental data, the distribution does not peak appropriately at $k = 2$, but instead at $k = 1$ indicating many pairs of bonds but no clusters. Instead, the peak of the distribution for $p = 0.3$ is most like the experimentally-observed distribution. A slightly larger value of p may be an artifact of under-sampling the number of minimally stressed particles that are hard to detect visually but do contribute stressed bonds. The distribution for $p = 0.3$ over-represents single bonds when compared with experiments, but the distribution of larger k values matches well. Alternately, since there is no reason to believe that accretion of bonds is independent of cluster size, we maybe seeing the result of bonds preferentially attaching to vertices of higher degree. Preferential attachment is often seen in complex networks [25].

Also plotted in Fig. 10 is the distribution for $p = 0.15$, below the measured p and not agreeing with the experimentally measured distributions. Finally, the distribution for $p = 0.5$, shows too much skew toward large clusters. Vertex degree is independent of the orientation of the lattice, so identical distributions are seen whether the lattice is oriented vertically or horizontally.

As indicated in Fig. 11, the q -Model gives a distribution of cluster size that falls linearly on a log-log plot until broadly peaking at roughly a quarter of the system size (100 vertices). Because we have chosen the critical case of the q -model to ensure long chains of contacts, it is not surprising that we see more large clusters. In contrast, the cluster size distribution for random graphs constructed from triangular lattices shown in Fig. 12 shows a power law with decreasing slope as p is increased. The slope for $p = 0.3$ is found to be most similar to that of the experimentally observed networks.

A sharp peak at the size of the system, indicating infinite clusters, is seen for the value $p = 0.5$. Similar “bi-modal” distributions were observed previously in bond percolation simulations with $N = 10^5$ [29].

Figure 13 shows the distribution of “weight” for the critical q -Model graphs. The distribution of weight in the actual q -Model is roughly similar to the q -Model-like weight assigned to the experimentally obtained graphs, however the model distribution is skewed towards large weights. This is unsurprising since, by construction, the critical q -Model is a connected graph. The distribution of upward trees in Fig. 14 is much broader than the weight distribution as discussed previously.

In Fig. 15, we have the distribution of weights assigned by the q -Model across downward pointing edges. None of the models showed the expected peak found in Fig. 7 for actual force networks. Random graphs composed from edges in vertically-aligned lattices — where an additional downward edge is possible — showed slightly broader distributions than those random graphs composed from horizontally-aligned triangular lattices. In the vertically-aligned lattices, the vertices with weight below the mean are distributed more broadly than in the horizontal case. For both alignments, the distribution for $p = 0.5$ was the most similar to the distribution for graphs obtained from experimental data —

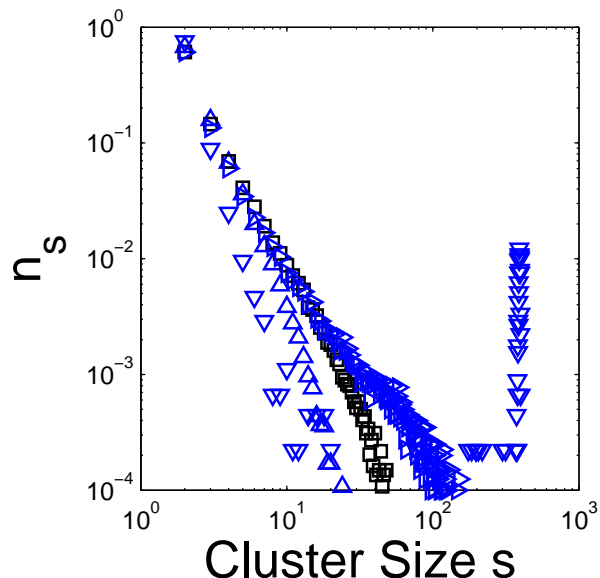


FIG. 12: The distribution of the number of clusters of size s from analyzing 500 realizations of random triangular graphs. The random graph results for the experimentally obtained $p = 0.2214$ are indicated by \square . Other bond probabilities, $p = 0.15$, 0.3 and 0.5 , are indicated by \triangle , \triangleright , and ∇ respectively. For all the modeled cases there is power law-like behavior over the size of the system. The slope varies non-monotonically for the random graph cases — decreasing as p is increased until abruptly dropping at $p = 0.5$. The second peak at large cluster size indicates that infinite clusters are forming. 0.5 is the transition value to universal clusters found by Matsuoka and greater than the critical probability $p_c = 0.3473$ for an infinite triangular lattice. For random graphs cluster size is independent of whether the basis is oriented horizontally or vertically.

this values is much larger than the p measured experimentally. None of these distributions can be said to match the force or q -Model distributions for experimentally obtained graphs.

As Fig. 16 shows, the only distributions of upward tree size that differ significantly are for random graphs constructed with $p = 0.5$ — where we observe infinite clusters. When there are vertical edges the distribution of cluster sizes is broader. This is reasonable since the addition of vertical edges makes large trees more likely. When comparing to the distribution found for experimentally-obtained graphs, however, there was too much noise to rule out any but the $p = 0.5$ distribution for random graphs with vertical edges.

Finally, we examine the robustness of our results. To obtain force network graphs from our experimental data in which the smaller particles were approximately 10 pixels in diameter, we convolved our images with a fringe kernel with a 7 pixel diameter. We used an acceptability threshold of 0.5, on a scale where 1.0 is a perfect match and 0.0 is the opposite of the kernel. As indicated by Fig. 17, varying the acceptability threshold has the slightly affects properties like vertex degree distribution without significantly changing the cluster size power law. Once the vertex locations were obtained, we assigned edges within the range $l = 13$ and we allowed a maximum of $k_{max} = 5$ edges. It is interesting to note that varying the threshold of acceptability is a rough experimental analog to previous numerical experiments [28].

VI. CONCLUSION

We have characterized the graphs generated from analyzing experimentally-obtained force networks in granular material. Assuming that each grain has four contacts, we calculate that the probability that a contact carries a large force is $p = 0.2214$. We propose that the geometry of force networks may be thought of as random sub-graphs of the contact network graph consisting of vertices at the particle centers and edges between each pair of touching particles. As indicated by the simulations of Matsuoka et al., (2001), the influence of factors such as the mobilization of friction on some aspects of the mean behavior of granular matter may perhaps be treated as graph problems.

To study this idea we have formed random graphs from sets of edges forming triangular lattices. We have found that different properties of the observed force networks can be matched depending upon a single parameter — the random chance for the presence of a bond. Though not all properties can be matched for one distinct bond probability p , the value of $p = 0.3$ worked for the graph-intrinsic properties of vertex degree and cluster size distribution. It is

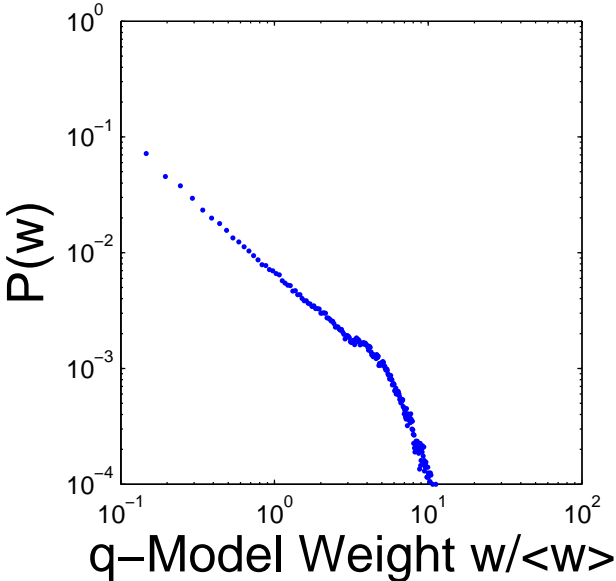


FIG. 13: Probability distributions determined from 500 realizations of the critical q -Model for weight assigned by the q -Model. Because there are far more vertices with weights below the mean, the distribution of q -Model weights is different from both the actual force and geometric q -Model weight distributions for experimentally obtained force networks.

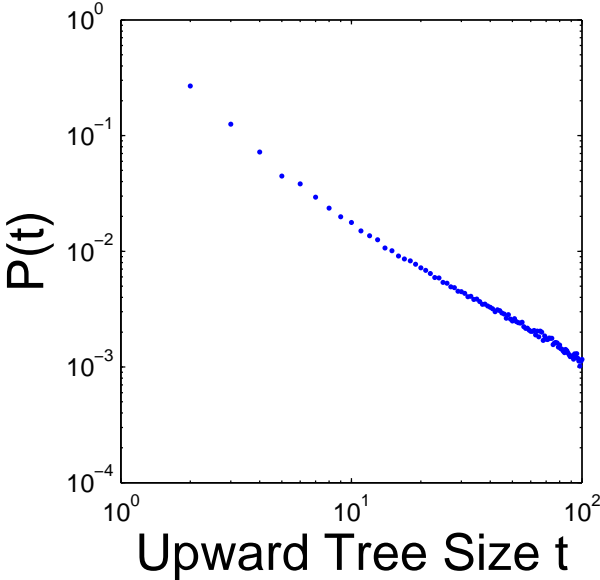


FIG. 14: Number distributions determined from 500 realizations of the critical q -Model for upward tree size.

possible that further refinement of the graph finding algorithm is needed to get the correct value of p for actual force networks. It is also possible that more sophisticated probabilistic methods are needed to account for features of other networks, such as preferential attachment of edges to vertices with higher degree.

Because of obvious similarities, we have made comparisons with the q -Model and attempted to assign weight to and determine force distribution of vertices in our graphs. Neither of the models for weight provide a clear match to the experimentally obtained results. This indicates that though graph theoretic approaches may in fact capture the geometry of force networks, the actual force distributions require more elaborate, vector analysis.

Finally, evidence for a well-defined bond probability p provides a physical basis for a Janssen-like parameter for describing the mobilization of friction of the contacts within the granular medium. When Coulomb's friction law is

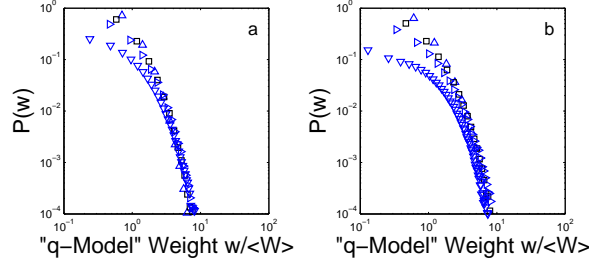


FIG. 15: Probability distribution of geometric q -Model weight from analyzing 500 realizations of random graphs assembled from horizontally- (a) and vertically- (b) aligned triangular lattices. The random graph results for the experimentally obtained $p = 0.2214$ are indicated by \square . Other bond probabilities, $p = 0.15, 0.3$ and 0.5 , are indicated by \triangle , \triangleright , and ∇ respectively. The two alignments differ in the distribution of vertices with less than the mean weight. The distribution of those edges is slightly broader for vertically-aligned lattices. In both cases, only the largest, $p = 0.5$, approaches the distribution observed for experimentally-obtained networks.

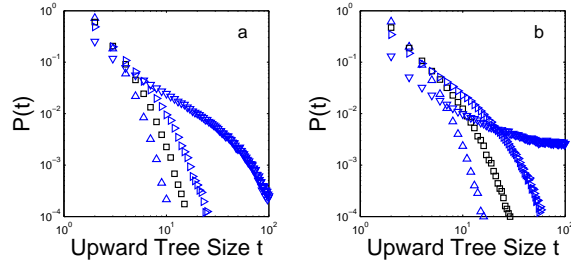


FIG. 16: Distribution of number of upward trees of size t from analyzing 500 realizations of random graphs assembled from horizontally- (a) and vertically- (b) aligned triangular lattices. The random graph results for the experimentally obtained $p = 0.2214$ are indicated by \square . Other bond probabilities, $p = 0.15, 0.3$ and 0.5 , are indicated by \triangle , \triangleright , and ∇ respectively. Only when infinite clusters are present ($p = 0.5$) do the distributions change significantly. The addition of vertical edges in **b** broadens the distribution since trees have a greater chance of being larger.

applied to spatially extended objects, the mean approach may perhaps not be thought of as a continuum, but rather an ensemble of random graphs.

Acknowledgements

I thank John Reif for suggesting the application of random graphs to force chain networks, Xiaobai Sun and Nikos Pitsianis for computer science advising; Richard Palmer, Josh Socolar, Brian Tighe and Trush Majmudar for helpful

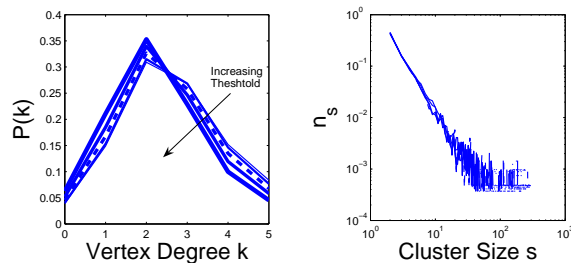


FIG. 17: **Left** Distribution of vertex degree for experimentally obtained force networks as a function of acceptability threshold for convolution with our fringe kernel. The dashed line indicates the acceptability threshold of 0.5 used for the analysis in this paper. Lowering the threshold from 0.6 (thickest line) to 0.4 (thinnest line) in increments of 0.05 increases the number of vertices “found” and skews the distribution away from chain-like structures towards higher vertex degree. **Right** Despite the change in vertex degree distribution, the distribution of cluster size still appears to be a power law with the same slope for all thresholds considered.

conversations and my advisor Robert Behringer. This research was funded by National Science Foundation grants DMR-0137119 and DMS-0204677 and NASA grant NNC04GB08G.

- [1] S. Roux and A. Hansen, in *Powders and Grains*, edited by J. Biarez and R. Gourvès (1989), pp. 249–254.
- [2] S. F. Edwards and D. V. Grinev, *Physica A* **294**, 545 (2001).
- [3] S. F. Edwards and R. B. S. Oakeshott, *Physica A* **157**, 1080 (1989).
- [4] R. Blumenfeld and S. F. Edwards, *Physical Review Letters* **90**, 114303 (2003).
- [5] M. Satake, in *Continuum Models of Discrete Systems*, edited by A. J. M. Spencer (1985), pp. 163–173.
- [6] J. Geng, D. Howell, E. Longhi, R. P. Behringer, G. Reydellet, L. Vanel, E. Clément, and S. Luding, *Physical Review Letters* **87**, 035506 (2001).
- [7] F. Radjai, D. Wolf, M. Jean, S. Roux, and J. Moreau, in *Powders and Grains*, edited by R. P. Behringer and J. T. Jenkins (1997), pp. 211–214.
- [8] M. E. Cates, J. P. Wittmer, J.-P. Bouchaud, and P. Claudin, *Physical Review Letters* **81**, 1841 (1998).
- [9] T. S. Majumdar and R. P. Behringer, *Nature* **435**, 1079 (2005).
- [10] K. Maeda, N. Kuwabara, and H. Matsuoka, in *Powders and Grains*, edited by Y. Kishino (2001), pp. 223–256.
- [11] S. N. Coppersmith, C. h. Liu, S. Majumdar, O. Narayan, and T. A. Witten, *Physical Review E* **53**, 4673 (1996).
- [12] J. Geng, G. Reydellet, E. Clément, and R. P. Behringer, *Physica D* **182**, 274 (2003).
- [13] P. Claudin, J.-P. Bouchaud, M. E. Cates, and J. P. Wittmer, *Physical Review E* **57**, 4441 (1998).
- [14] J. E. S. Socolar, *Physical Review E* **57**, 3204 (1997).
- [15] S. F. Edwards and D. V. Grinev, *Physical Review Letters* **82**, 5397 (1999).
- [16] K. Bagi, in *Powders and Grains*, edited by R. P. Behringer and J. T. Jenkins (1997), pp. 251–254.
- [17] J. D. Goddard, *International Journal of Solids and Structures* **41**, 5851 (2004).
- [18] J. E. S. Socolar, D. G. Schaeffer, and P. Claudin, *Euro. Phys. J. E* **7**, 353 (2002).
- [19] J. H. Snoeijer, T. J. H. Vlugt, M. van Hecke, and W. van Saarloos, *Physical Review Letters* **92**, 054302 (2004).
- [20] J. Park and M. E. J. Newman, *Physical Review E* **70**, 066117 (2004).
- [21] M. F. Sykes and J. W. Essam, *Journal of Mathematical Physics* **5**, 1117 (1964).
- [22] D. S. Callaway, M. E. J. Newman, S. H. Strogatz, and D. J. Watts, *Physical Review Letters* **85**, 5468 (2000).
- [23] N. Alon and J. H. Spencer, *The Probabilistic Method* (John Wiley and Sons, 2000).
- [24] D. J. Watts and S. H. Strogatz, *Nature* **393**, 440 (1998).
- [25] R. Albert and A.-L. Barabási, *Reviews of Modern Physics* **74**, 47 (2002).
- [26] J. S. Andrade, H. J. Herrmann, R. F. S. Andrade, and L. R. da Silva, *Physical Review Letters* **94**, 018702 (2005).
- [27] S. Ostojic and B. Nienhuis, in *Traffic and Granular Flow* (2005).
- [28] S. Ostojic, E. Somfai, and B. Nienhuis, *Nature* **439**, 828 (2006).
- [29] L. K. Gallos and P. Argyrakis, *Physica A* **330**, 117 (2003).